DOI:10.1021/jf900337h

JOURNAL OF AGRICULTURAL AND FOOD CHEMISTRY
ARTICLE

Mycobased Synthesis of Silver Nanoparticles and Their Incorporation into Sodium Alginate Films for Vegetable and Fruit Preservation

A. Mohammed Fayaz,*,† K. Balaji,§ M. Girilal,† P. T. Kalaichelvan,† and R. Venkatesan#

†CAS in Botany, University of Madras, Guindy Campus, Chennai, India, §Orchid Healthcare, A Division of Orchid Chemicals and Pharmaceuticals Ltd., Chennai, India, and #South Asia Co-operative Environment Programme, Colombo, Sri Lanka

Biosynthesis of silver nanoparticles using *Trichoderma viride* and their incorporation into sodium alginate for vegetable and fruit preservation has been demonstrated in this study. Aqueous silver (Ag^+) ions when exposed to the filtrate of *T. viride* are reduced in solution. These extremely stable silver nanoparticles were characterized by means of UV−vis spectrophotometer, FTIR, TEM, and EDS. The nanoparticles exhibit maximum absorbance at 421 nm in the UV spectrum. The presence of proteins was identified by FTIR. TEM micrograph revealed the formation of polydispersed nanoparticles, and the presence of elemental silver was confirmed by EDS analysis. The silver nanoparticle incorporated sodium alginate thin film shows good antibacterial activity against test strains. This film increases the shelf life of carrot and pear when compared to control with respect to weight loss and soluble protein content. These results show silver nanoparticle incorporated sodium alginate coated vegetables and fruits are suitable for preservation.

KEYWORDS: Antibacterial activity; biogenic; preservation; shelf life; silver nanoparticles

INTRODUCTION

In many agriculture-based countries, the main problem is to keep the fruits and vegetables safe and fresh until they reach the consumers' hands. Even though the fruits and vegetables have a natural waxy coating, it is not adequate to offer protection against water loss and high respiration rate, thus resulting in weight and protein losses during storage. The U.S. Centers for Disease Control and Prevention estimates around 76 million cases of foodborne illness in the United States each year, resulting in about 5000 deaths (*1*). Edible coatings and films are currently used on a wide variety of foods, including fruits, vegetables, meats, chocolates, candies, bakery products, and French fries (*2*−*5*). The basic functional properties of edible coatings and films depend on the characteristics of the film-forming materials used for their preparation. At present, the primary film-forming materials used to construct edible coatings and films are polysaccharides, proteins, and lipids. Generally, lipid-based films are good moisture barriers, but they offer little resistance to gas transfer and have poor mechanical strength. In contrast, biopolymer-based films are often good oxygen and carbon dioxide barriers, but they offer little protection against moisture migration (*6*).

Edible coatings or films could serve as moisture, lipid, and gas barriers. Alternatively, they could improve the textural properties of food or serve as carriers of functional agents such as colors, flavors, antioxidants, nutrients, and antimicrobials. Different microorganisms are responsible for the spoilage of fruits and vegetables, thus decreasing their quality and shelf life. In recent years, the antimicrobial coating process without the use of preservative has been gaining more importance in controlling and preventing foodborne microbial outbreaks. A number of naturally occurring enzymes such as lysozymes, lactoperoxidases, and glucose oxidase have also been used as antimicrobial agents for food preservations (*7*). The main drawbacks of these enzymes are their lower stability and activity unless maintained at their optimum conditions (pH and temperature).

The use of protective nanocoating and suitable packaging has become a topic of great interest in the field of food nanotechnology because of their potential for increased shelf life of many food products (*8*). Over the past decade, there has been a strong push toward the development of silver-containing materials for commercial use that exhibit antimicrobial or bactericidal properties. Silver nanoparticles have a broad spectrum of antibacterial activity against Gram-negative and Gram-positive bacteria, and there is also minimal development of bacterial resistance (*9*). Because chemical synthesis methods produce a toxic substance as byproduct, there was a big challenge to develop a new protocol that is a reliable, green chemistry process for the synthesis of nanoparticles that does not use toxic chemicals in the synthesis protocols. Recently, scientists have looked to microorganisms as possible ecofriendly nanofactories for the synthesis of nanoparticles (*10*), such as CdS (*11*), gold (*12*), and silver (*13*).

*Address correspondence to this author at CAS in Botany, University of Madras, Guindy Campus, Chennai 600 025, India [telephone (91) 9884466583; fax + (91)-44-2352494; e-mail nanofayaz@gmail.com].

 Published on Web 06/24/2009

In the present study, we synthesized biogenic silver nanoparticles using *Trichoderma viride* and demonstrated that silver nanoparticles incorporated with polysaccharide films along with glycerol give both surface protection and antibacterial edible coating for vegetables and fruits. This prevents weight loss and protein loss and also precludes microbial spoilage, thus increasing the shelf life of vegetables and fruits. To our best knowledge this is the first report of biogenic silver nanoparticles incorporated with polysaccharide film used for vegetable and food preservation.

MATERIALS AND METHODS

Chemicals. Silver nitrate was obtained from Merck (Darmstadt, Germany). Sodium alginate, ethanol, chlorine dioxide, glycerol, potassium dihydrogen phosphate, dipotassium hydrogen phosphate, magnesium sulfate heptahydrate, and ammonium sulfate were from SRL (Mumbai, India). Glucose was from Rankem (Mumbai, India) and Muller−Hinton agar from Himedia (Mumbai, India).

Carrot and Pear. Carrots (*Daucus carota*) were procured from a local supermarket at 75 days of sowing; length ranged from 10 to 12 cm, and average weight ranged from 80 to 120 g. Pears (*Pyrus communis*) were harvested at 25 days after flowering. The size of the pears ranged from 6 to 8 cm in height, and weight ranged from 250 to 300 g.

Microorganisms and Culture Media. The fungus *Trichoderma viride* was obtained from the Culture Collection Center, CAS in Botany, University of Madras, India, and maintained in potato dextrose agar slant at 27 °C. Pure cultures of *Escherichia coli* ATCC 8739 (Gram-negative rods) and *Staphylococcus aureus* ATCC 6538 (Gram-positive cocci) were obtained from American Type Culture Center, and the species level confirmations for all microorganisms were identified using the microbial identification system bioMèrieux, mini API, Italy.

Production of Biomass. To prepare the biomass for biosynthesis studies the fungus was grown aerobically in liquid broth containing dihydrogen potassium phosphate (7 g/L), dipotassium hydrogen phosphate (2 g/L), magnesium sulfate heptahydrate (0.1 g/L), ammonium sulfate (1 g/L), yeast extract (0.6 g/L), and glucose (10 g/L). The culture flasks were incubated on an orbital shaker at 27 °C and agitated at 150 rpm, and the biomass was harvested after 72 h of growth by sieving through a plastic sieve, followed by extensive washing with sterile double-distilled water to remove any medium components from the biomass.

Synthesis of Silver Nanoparticles. Typically, 20 g (wet weight of biomass) was brought into contact with 100 mL of sterile double-distilled water for 48 h at 27 °C in an Erlenmeyer flask and agitated as described earlier. After the incubation, the cell filtrate was filtered by Whatman filter paper no. 1. To 100 mL of cell filtrate was added to the Erlenmeyer flask a carefully weighed quantity of silver nitrate to yield an overall Ag^+ ion concentration of 10^{-3} M, and the reaction was carried out in the dark.

Characterization of Silver Nanoparticles. Surface plasmon resonance of silver nanoparticles was characterized using a UV−vis spectrophotometer (Cary 300 Conc spectrophotometer) at the resolution of 1 nm from 250 to 800 nm. For transmission electron microscopy (TEM), the sample was prepared by a drop of colloidal solution of nanosilver on a carbon-coated copper grid and setting a completely dried drop by vacuum desiccator. The image of the sample was obtained using a transmission electron microscope (JEOL 2000 FX MARK II) equipped with an EDX attachment. The FTIR spectrum of the sample was recorded by Perkin-Elmer Fourier transform infrared spectroscopy; the spectrum ranged from 2000 to 1000 cm^{-1} at a resolution of 4 cm^{-1}, by making a KBr pellet with silver nanoparticles.

Analysis of Antibacterial Activity of Silver Nanoparticles against *E. coli* ATCC 8739 and *S. aureus* ATCC 6538 Test Strains. The effect of silver nanoparticles on Gram-positive and Gram-negative bacteria was investigated by liquid broth dilution method (*14*). The cultures were inoculated from fresh colonies on agar plates into 100 mL Luria−Bertani (LB) culture medium. The growth of *E. coli* ATCC 8739 was allowed until the optical density reached 0.2 at 600 nm (OD of 0.2 corresponds to a concentration of 10^8 CFU mL^{-1} of medium). Subsequently, 2×10^8 CFU culture from above was added to 100 mL of LB media supplemented with 10, 20, 30, and 40 μg/mL of silver nanoparticles, whereas medium without nanoparticles was used as control. Growth rate was determined by measuring optical density at 600 nm at regular intervals. To define further the effect of silver nanoparticles on Gram-positive bacteria, *S. aureus* ATCC 6538 test strain was exposed to higher doses of silver nanoparticles (50, 60, 70, and 80 μg/mL) and the growth was studied.

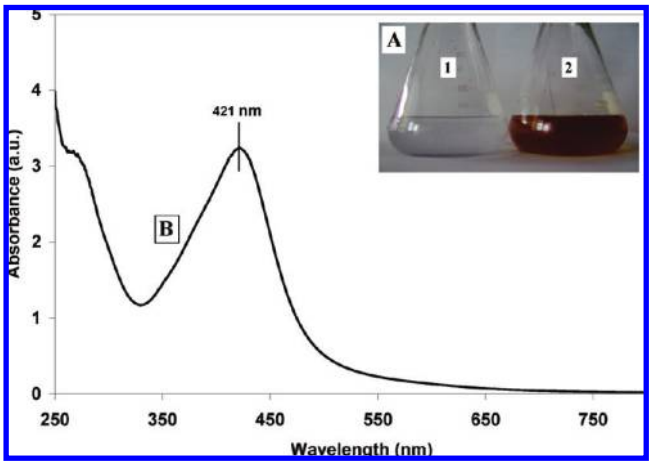

Figure 1. (**A**) Picture of flask containing the solution of *T. viride* cell filtrate with 10^{-3} M of silver nitrate in Erlenmeyer flask, before reaction (flask 1) and after 24 h of reaction (flask 2). (**B**) UV−visual absorption spectra of silver nanoparticles after 24 h of reaction.

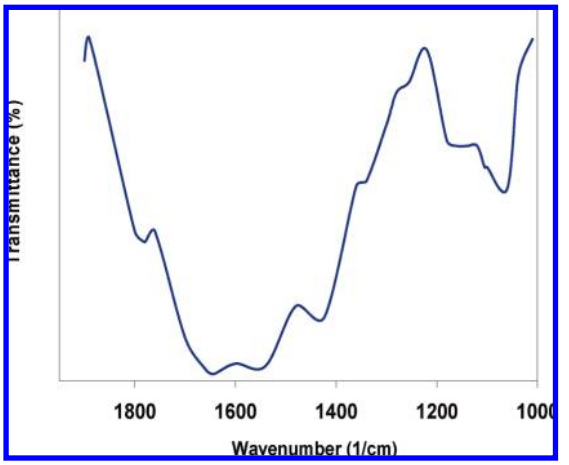

Figure 2. FTIR spectrum recorded by making a KBr pellet with synthesized silver nanoparticles.

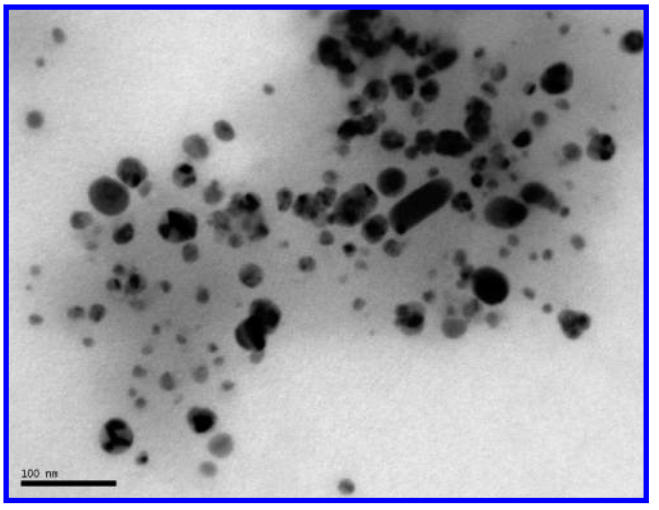

Figure 3. Bright field TEM micrograph of biogenic synthesized silver nanoparticles.

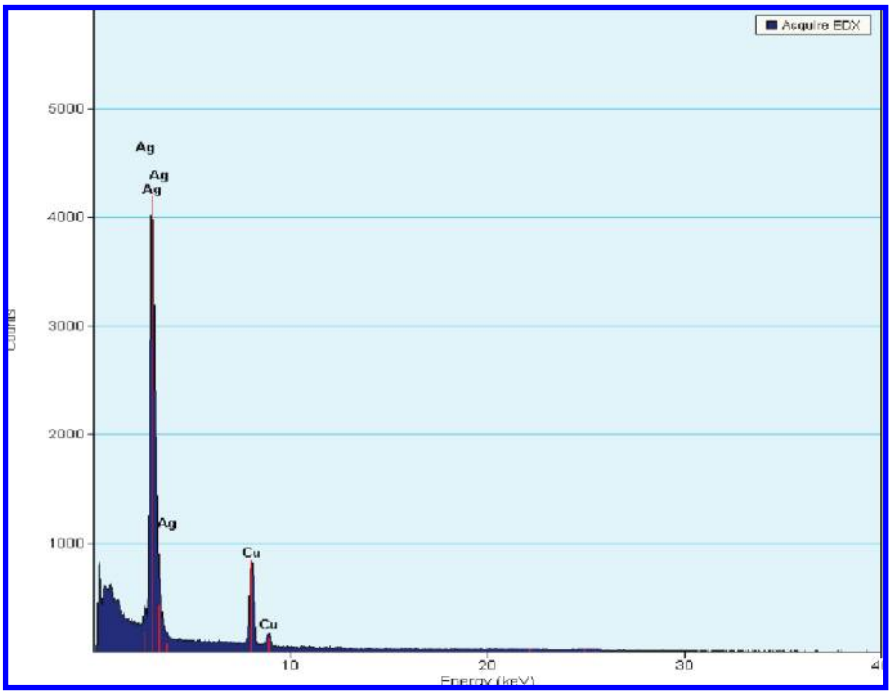

Figure 4. EDS spectrum of silver nanoparticles. Different X-ray emission peaks showing strong signals from the atoms in the silver nanoparticles are observed, whereas weaker signals from Cu atoms are also visible.

Silver Nanoparticle Incorporated Sodium Alginate Film Preparation. Sodium alginate was weighed to 2.5 g and dissolved in 25 mL of glass-distilled water by mixing slowly with a magnetic stirrer for 30 min; 1 mL of glycerol was added to the medium, and the temperature of the mixture was increased until it started to boil. Mixing was then ceased, and the solution was boiled for 5 min. After the mixture had cooled to room temperature, silver nanoparticles (80 μg/mL) were added to it. This mixture was further stirred for 20 min and then spread evenly onto a glass plate, which had been previously cleaned and wiped with ethanol. The plates were placed in an incubator, and the thin film was dried at room temperature for 24 h. After drying, the films were cut into small pieces and checked for antibacterial activity.

Antibacterial Activity of Silver Nanoparticle Incorporated Sodium Alginate Films. A disk diffusion method was used to assay the antibacterial activity of silver nanoparticle incorporated sodium alginate thin film against test strains on Muller−Hinton agar plates. A single colony of each test strain was grown overnight in Muller−Hinton liquid medium on a rotary shaker (at 200 rpm) at 35 °C. The inocula were prepared by diluting the overnight cultures with 0.9% NaCl to a 0.5 McFarland standard and were applied to the plates along with the silver nanoparticle incorporated sodium alginate thin film and sodium alginate film without silver nanoparticles. After incubation at 37 °C for 24 h, the zones of inhibition were observed.

Surface Sterilization of Fruits and Vegetables. Fresh fruits and vegetables were purchased from a local supermarket and stored at 4 °C before processing. In this study, chlorine dioxide has been chosen for surface sterilization of fruits and vegetables. The concentration of ClO_2 and soaking time were optimized for efficient and minimal use of chlorine dioxide.

Film Coating Procedure. Carrots and pears were surface-sterilized with chlorine dioxide (6 ppm) for 20 min. Surface-sterilized whole carrots and pears were taken for sodium alginate coating with silver nanoparticles. Fresh carrots and pears were immersed completely into the coating solution for 5 s at room temperature and then taken out. The same procedure was repeated twice, and excess coating was allowed to drain completely. Then the coating was dried in an air blower. Coated and uncoated carrots and pears were kept at 27 °C before the analysis of loss of water and protein content.

Determination of Weight Loss and Soluble Protein Content. Protein estimation was done using bovine serum albumin fraction V (Sigma Chemicals Co.) as standard. The water loss (weight loss) and soluble protein content were monitored regularly in carrots and pears stored at room temperature (27 °C), which had already been weighed, packed, and kept in perforated polypropylene covers. They were weighed every 2 days to determine weight loss. Soluble protein content was estimated by using Bradford's method (*15*). The carrots and pears were weighed to about 0.1 g, mixed with 2 mL of distilled water, and homogenized for 5 min at room temperature. The tubes were centrifuged at 5000 rpm for 20 min. The supernatant was collected in Eppendorf tubes and stored at 4 °C for 2 h before analysis. The protein extract was diluted 50 times, and from that 1.0 mL of protein extract was mixed with 5 mL of Coomassie brilliant blue G-250 (100 mg) and incubated for 15 min at room temperature; the absorbance was read at 595 nm using a spectrophotometer.

Sensory Analysis. Sensory analysis was performed using five members of a trained panel with an age range of 21−30 years. The panel consists of three females and two males with sensory evaluation experience, and they were trained in discriminative evaluation of vegetables and fruits. Treated pears and carrots along with controls kept at 27 °C were considered for sensory analysis; assessment was carried out for 10 days at 2 day intervals. The samples were screened for overall acceptance (color, appearance, texture, aftertaste). The panelists relied on their training experience to evaluate products.

Statistical Analysis. All values are expressed as means ± standard deviation. The results were analyzed using one-way analysis of variance (ANOVA), and the differences among the formulation means were analyzed using the Tukey−Kramer multiple-comparison test. A P value of < 0.001 was considered to be significant. The software GraphPad InStat was employed for the statistical analysis.

RESULTS AND DISCUSSION

The study on the extracellular biogenic synthesis of silver nanoparticles by *T. viride* was carried out and demonstrated that silver nanoparticles incorporated into sodium alginate films along with glycerol could be used for vegetable and fruit preservation.

Surface Plasmon Resonance of Reduced Silver Nanoparticles. Aqueous silver nitrate ions were reduced during exposure to the *T. viride* culture filtrate. The color of the reaction mixture changed from colorless to brown as shown in **Figure 1A**, which indicated the formation of silver nanoparticles. It is well-known that silver nanoparticles exhibit yellowish brown color in water

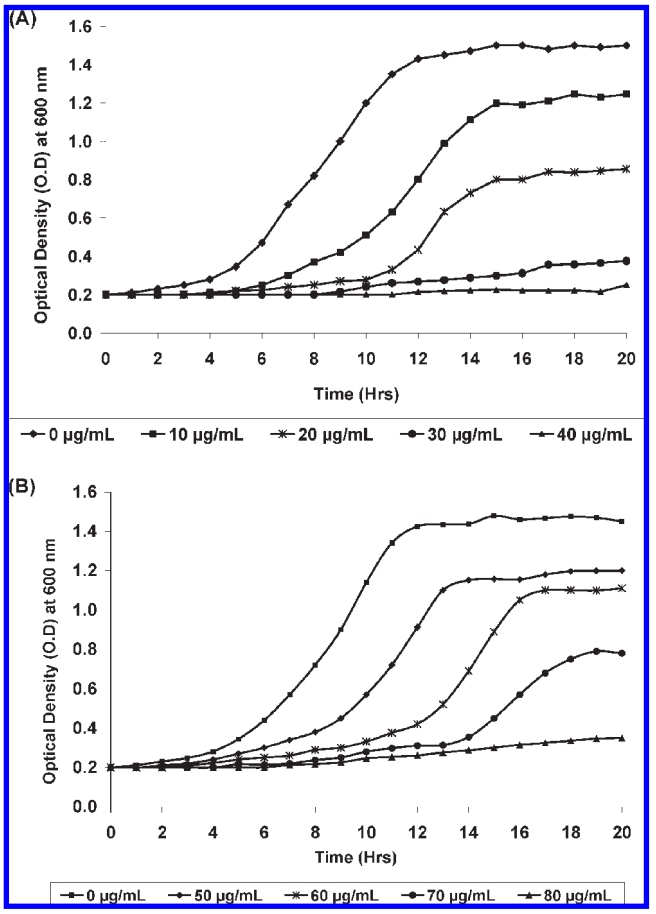

Figure 5. Bacterial growth inhibition curves in LB media at different concentrations of silver nanoparticles: (**A**) *E. coli* ATCC 8739; (**B**) *S. aureus* ATCC 6538.

Table 1. Optimization of Time and Dosage of Chlorine Dioxide for Surface Sterilization

incubation time (min)	CFU/mL				
	2 ppm ClO_2	4 ppm ClO_2	6 ppm ClO_2	8 ppm ClO_2	10 ppm ClO_2
10	32	14	7	3	
20	20	8			
30	11	3			

due to excitation of surface plasmon vibration in metal nanoparticles (*16*). The excitation spectra of the silver nanoparticle samples were characterized by UV−visible spectroscopy, and this technique has proved to be very useful for the analysis of nanoparticles (*17*). **Figure 1B** shows the strong surface plasmon resonance centered at ca. 421 nm, which indicates the formation of silver nanoparticles extracellularly; an absorbance band at 270 nm is also clearly visible and is attributed to aromatic amino acids of proteins. It is well-known that the absorbance band at 270 nm arises due to electronic excitation in tryptophan and tyrosine in the proteins (*18*).

Identification of Functional Groups by FTIR. The spectrum of extracellular biosynthesized silver nanoparticles is shown in **Figure 2**. The spectrum shows the presence of bands at 1650, 1540, 1423, and 1060 cm^{-1}. The band at 1650 cm^{-1} corresponds to a primary amine NH band; similarly, bands at 1540 and 1060 cm^{-1} correspond to a secondary amine NH band and a primary amine CN stretch vibration of the protein, respectively (*19*). The positions of these bands were close to those reported for native proteins; the FTIR results indicate that the

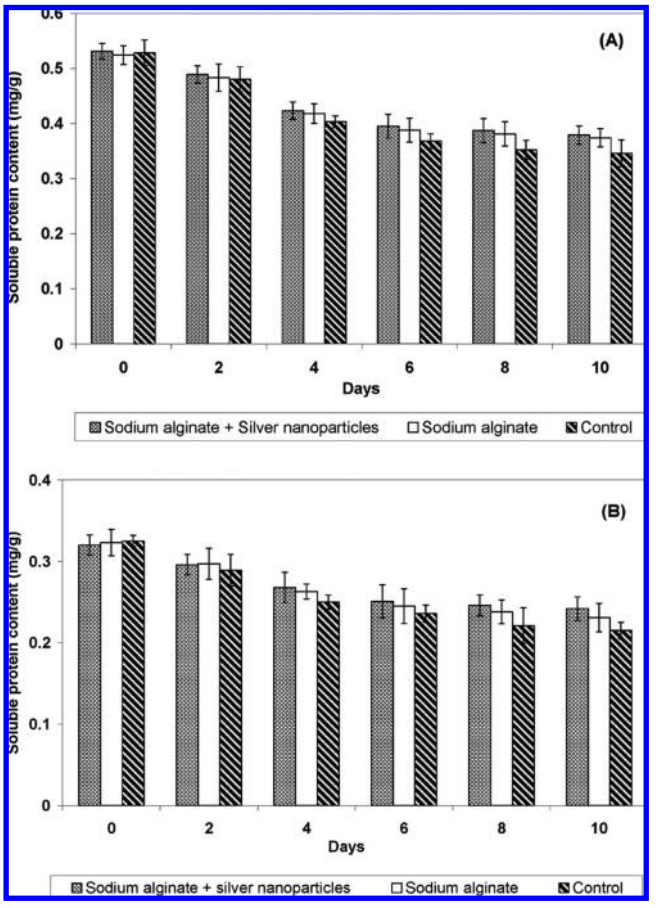

Figure 6. Soluble protein content in silver nanoparticle incorporated sodium alginate film coated carrot (**A**) and pear (**B**).

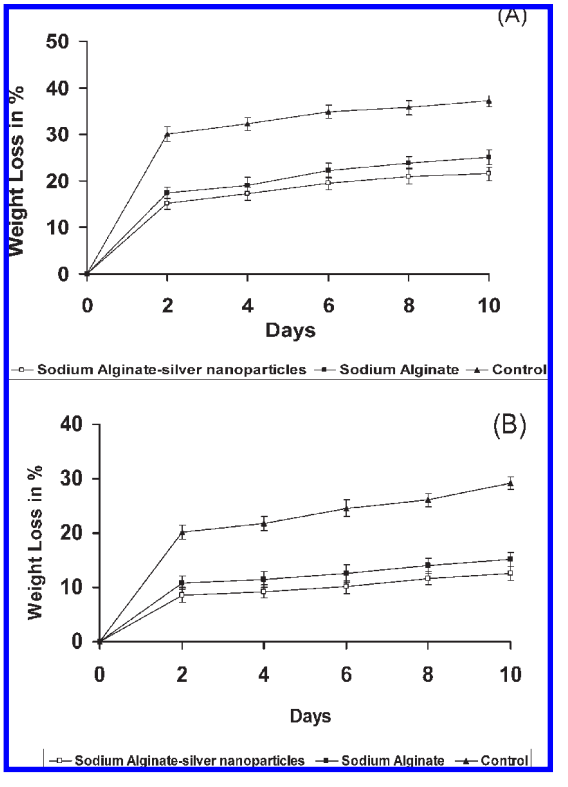

Figure 7. Percentage of weight loss in silver nanoparticle incorporated sodium alginate film coated carrot (**A**) and pear (**B**).

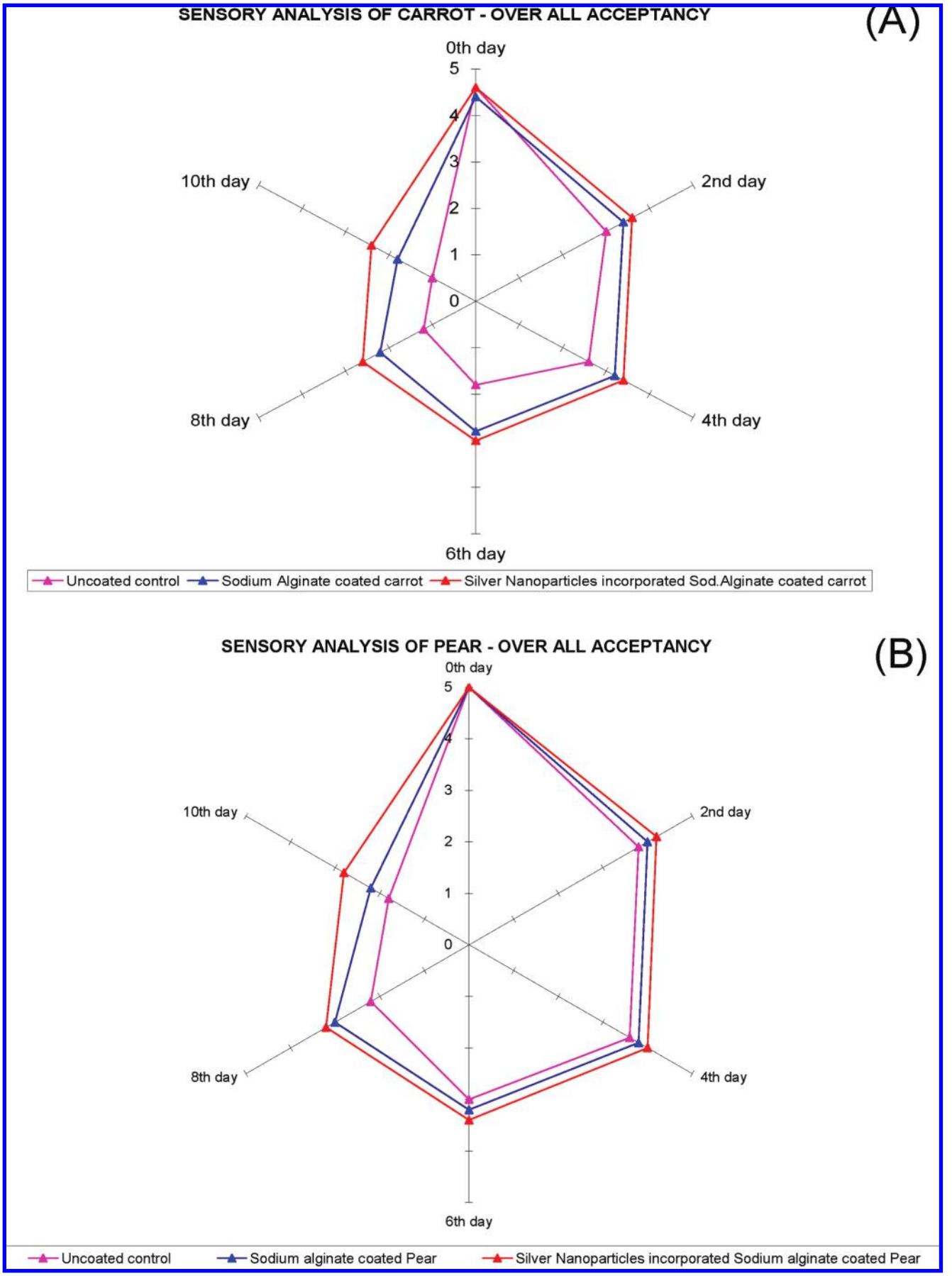

Figure 8. Sensory analysis of overall acceptance: carrot (**A**) and pear (**B**).

secondary structures of proteins were not affected as a consequence of reaction with Ag^+ ions or binding with silver nanoparticles. The band at 1425 cm^{-1} is assigned to a methylene scissoring vibration from the protein in the solution (*20*). This evidence suggests that the release of extracellular protein molecules could possibly perform the function for the formation and stabilization of silver nanoparticles in aqueous medium.

Transmission Electron Microscopy. A TEM micrograph recorded from the silver nanoparticle film deposited on a carbon-coated copper TEM grid is shown in **Figure 3**. This micrograph shows spherical and occasionally rodlike silver nanoparticles. It is observed from the micrograph that most of silver nanoparticles are in the range of 5−40 nm in size. The additional support of reduction of Ag^+ ions to elemental silver was confirmed by EDS analysis. The optical absorption peak is observed approximately at 3 keV, which is typical for the absorption of metallic silver nanocrystalline due to surface plasmon resonance, which confirms the presence of nanocrystalline elemental silver, which is shown in **Figure 4**.

Antibacterial Activity of Silver Nanoparticles against Gram-Positive and Gram-Negative Bacteria. The bacterial growth inhibition curves for extracellular biosynthesized silver nanoparticles on Gram-positive and Gram-negative bacteria were determined by the broth dilution method (*21*). In this experiment *E. coli* ATCC 8739 and *S. aureus* ATCC 6538 test strains were inoculated in LB medium supplemented with silver nanoparticles. Increasing concentration of silver nanoparticles substantially inhibits the growth of *E. coli* ATCC 8739 test strain as shown in **Figure 5A**. The lag phase was found to be more prolonged than described by others (*22*). This could be attributed to greater antibacterial effect of nanoparticles against the *E. coli* ATCC 8739 test strain. The concentration of 40 μg/mL was found to possess a strongly antibacterial activity against *E. coli* ATCC 8739 test strain as it took about 11 h to initiate any noticeable growth. In the same time, silver nanoparticles were found to have a less significant effect on the growth of Gram-positive bacteria (*S. aureus* ATCC 6538 test strain). The concentration of 80 μg/mL elicited 80% growth inhibition, which is shown in **Figure 5B**.

Antibacterial Activity of Silver Nanoparticle Incorporated Sodium Alginate Films. In the present study, antibacterial activities of silver nanoparticle incorporated sodium alginate films were tested against *E. coli* ATCC 8739 and *S. aureus* ATCC 6538 test strains. A clear zone was observed around the silver nanoparticle incorporated sodium alginate film, whereas it was not observed around the control film. This clearly shows that the silver nanoparticle incorporated sodium alginate film retains its antibacterial activity against both Gram-positive and Gram-negative organisms after coating.

Surface Sterilization of Carrots and Pears. Chlorine dioxide was optimized against dosage and time interval, and it was observed that significant inhibitory activity was found at 6 ppm for 20 min. The plate count readings are given in **Table 1** in terms of CFU per milliliter. Chlorine dioxide had received a lot of attention in the past few years because its effectiveness is less affected by pH and organic matter content than that of chlorine. Another advantage is its high oxidation action, which has been observed to be 2.5 times greater than that of chlorine (*23*).

Measurement of Soluble Protein Content. There was no significance difference in soluble protein content during the storage period. The initial soluble protein contents of silver nanoparticle incorporated sodium alginate film coated carrots and pears were 0.531 ± 0.014 and 0.32 ± 0.024 mg/g of dry wt, respectively, which dropped significantly and reached their lowest values of 0.379 ± 0.017 and 0.242 ± 0.015 mg/g of dry wt, respectively, which is shown in **Figure 6**. The decrease in soluble protein content between 2 and 6 days is due to utilization of soluble protein for metabolic activities such as substrate for respiration, due to inadequate carbohydrate source (*24*).

Measurement of Weight Loss in Percentage. Silver nanoparticle incorporated sodium alginate film coated carrots and pears were observed to have minimum weight loss compared to sodium alginate coated and uncoated control, which is shown in **Figure 7**. Sodium alginate film with glycerol prevents water loss. There was a drastic increase in water loss for the first 2 days, and then the water loss stabilized and increased relatively slowly, until the 10th day. The loss of water is a natural process of the catabolism in fresh-cut vegetables and is attributed to the respiration and other senescence-related metabolic processes during storage (*25*).

Sensory Assessment. The overall acceptability for uncoated control, sodium alginate coated, and silver nanoparticle incorporated sodium alginate coated carrots and pears is represented in **Figure 8**. Silver nanoparticle incorporated sodium alginate coated carrots and pears were acceptable at up to 10 days of storage, as judged by the color and appearance, texture, and aftertaste compared to uncoated control and sodium alginate coated carrots and pears. There was no overall acceptance for sodium alginate coated carrots and pears after the 6th and 8th days of storage, respectively. This may be caused by gradual increase in the microbial infection in sodium alginate coated carrots and pears, which reduces their acceptance.

These results reinforce the ecofriendly protocol for synthesis of biogenic silver nanoparticles and the novel method for vegetable and food preservation using biogenic silver nanoparticle incorporated sodium alginate films. This work provides a new approach to utilize the nanobiotechnology field for food preservation.

ABBREVIATIONS USED

Ag-NPs, silver nanoparticles; EDS, energy-dispersed spectroscopy; FTIR, Fourier transforms infrared spectroscopy; TEM, transmission electron microscopy; CFU, colony-forming units.

ACKNOWLEDGMENT

We thank Prof. R. Rengasamy, Director, CAS in Botany, University of Madras, for providing adequate laboratory facility to carry out this research work.

LITERATURE CITED

(1) Mead, P. S.; Slutsker, L.; Dietz, V.; McCaig, L. F.; Bresee, J. F.; Shapiro, C.; et al. Food-related illness and death in the United States. *Emerging Infectious Dis.* **1999**, *5* (5), 607–625.

(2) Morillon, V.; Debeaufort, F.; Blond, G.; Capelle, M.; Voilley, A. Factors affecting the moisture permeability of lipid-based edible films: a review. *Crit. Rev. Food Sci. Nutr.* **2002**, *42*, 67–89.

(3) Cagri, A.; Ustunol, Z.; Ryser, E. T. Antimicrobial edible films and coatings. *J. Food Prot.* **2004**, *67*, 833–848.

(4) Cha, D. S.; Chinnan, M. S. Biopolymer-based antimicrobial packaging: review. *Crit. Rev. Food Sci Nutr.* **2004**, *44*, 223–237.

(5) Rhim, J. W. Increase in water vapor barrier property of biopolymer-based edible films and coatings by compositing with lipid materials. *J. Food Sci. Biotechnol.* **2004**, *13*, 528–535.

(6) Jochenweiss, P. T.; McClements, D. J. Functional materials in food nanotechnology. *J. Food Sci.* **2006**, *71*, 107–116.

(7) Davidson, P. M. Chemical preservatives and natural antimicrobial compounds. In *Food Microbiology Fundamentals and Frontiers*; Doyle, M. P., Beuchat, L. R., Montville, T. J., Eds.; ASM Press: Washington, DC, 2001; pp 593−627.

(8) Ahvenainen, R. *Novel Food Packaging Techniques*; CRC Press: Boca Raton, FL, 2003.

(9) Ip, M.; Lui, S. L.; Poon, V. K. M.; Lung, I.; Burd, A. *J. Med. Microbiol.* **2006**, *55*, 59−63.
(10) Bolander, M. E.; Mukhopadhyay, D.; Sarkar, G.; Mukherjee, P. The use of microorganisms for the formation of metal nanoparticles and their application. *Appl. Microbiol. Biotechnol.* **2006**, *69*, 485–492.
(11) Ahmad, A.; Mukherjee, P.; Mandal, D.; Senapati, S.; Islam Khan, M.; Rajiv Kumar; Sastry, M. Enzyme mediated extracellular synthesis of CdS nanoparticles by the fungus, *Fusarium oxysporum*. *J. Am. Chem. Soc.* **2002**, *124*, 12108–12109.
(12) Mukherjee, P.; Senapati, S.; Mandal, D.; Ahmad, A.; Khan, M. I.; Kumar, R.; Sastry, M. Extracellular synthesis of gold nanoparticles by the fungus *Fusarium oxysporum*. *Chem. Biochem.* **2002**, *3*, 461–463.
(13) Ahmad, A.; Mukherjee, P.; Senapati, S.; Mandal, D.; Khan, M. I.; Kumar, R.; Sastry, M. Extracellular biosynthesis of silver nanoparticles using the fungus *Fusarium oxysporum*. *Colloids Surf. B* **2003**, *28*, 313–318.
(14) Shrivastava, S.; Tanmay, B. E.; Roy, A.; Singh, G.; Ramachandra Rao, P.; Dash, D. Characterization of enhanced antibacterial affects of novel silver nanoparticles. *Nanotechnolgy* **2007**, *18*, 225103.
(15) Bradford, M. A rapid and sensitive method for the quantification of protein using the principle of protein−dye binding. *Anal. Biochem.* **1976**, *72*, 248–254.
(16) Ahmad, A.; Senapati, S.; Islam Khan, M.; Kumar, R.; Ramani, R.; Srinivas, V.; Sastry, M. Intracellular synthesis of gold nanoparticles by a novel alkalotolerant actinomycete, *Rhodococcus* species. *Nanotechnology* **2003**, *14*, 824–828.
(17) Muvaney, P. Surface plasmon spectroscopy of nanosized metal particles. *Langmiur* **1996**, *12*, 788–800.
(18) Eftink, M. K.; Ghiron, C. A. Fluorescence quenching studies with proteins. *Anal. Biochem.* **1981**, *114*, 199–227.
(19) Madigan, M.; Martinko, J. *Brock Biology of Microrganisms*, 11th ed.; Prentice Hall: Englewood Cliffs, NJ, 2005.
(20) Macdonald, I. D.G.; Smith, W. E. Orientation of cytochrome C adsorbed on a citrate-reduced silver colloid surface. *Langmuir* **1996**, *12*, 706–713.
(21) Shrivastava, S.; Tanmay, B. E.; Roy, A.; Singh, G.; Ramachandra Rao, P.; Dash, D. Characterization of enhanced antibacterial affects of novel silver nanoparticles. *Nanotechnolgy* **2007**, *18* (225103), 1–9.
(22) Sondi, I.; Salopek-Sondi, B. Silver nanoparticles as antimicrobial agent: a case study of *E. coli* as a model for Gram-negative bacteria. *J. Colloids Interface Sci.* **2004**, *275*, 177–182.
(23) Benarde, M. A.; Snow, W. B.; Olivieri, P.; Davidson, B. Kinetics and mechanism of bacterial disinfection by chlorine dioxide. *Appl. Microbiol.* **1967**, *15*, 2167.
(24) King, G. A.; Woollard, D. C.; Irving, D. E.; Borst, W. M. Physiological changes in asparagus spears tips after harvest. *Physiol. Plant.* **1990**, *80*, 393–400.
(25) Watads, A. E.; Qui, L. Quality of fresh-cut produce. *Postharvest Biol. Technol.*

Received for review January 30, 2009. Revised manuscript received June 2, 2009. Accepted June 9, 2009. We thank the UGC for providing the scholarship through UGC Research Fellowship in Science for Meritorious Students.